AIChE

Several Basic and Practical Aspects Related to Electrochemical Deionization of Water

Yaniv Bouhadana, Eran Avraham, Abraham Soffer, and Doron Aurbach
Dept. of Chemistry, Bar Ilan University, Ramat-Gan, Israel

DOI 10.1002/aic.12005
Published online October 22, 2009 in Wiley InterScience (www.interscience.wiley.com).

We examine water desalination processes based on the electrosorption of ions onto activated carbon electrodes (capacitive deionization, CDI). A flow-by operation mode was used (solutions flows within channels in the separator, parallel to the electrodes) in both continuous and stopped flow experiments. The different response of solutions containing more than 5000 ppm NaCl and dilute solutions (e.g., 1000 ppm NaCl) to the applied potential is discussed. The electrical current transients on potential steps were faster by two orders of magnitude than the resulting concentration transients due to the dynamics of these deionization processes and the properties of the cells used herein. Guidelines for the practical development of capacitive water deionization processes are discussed herein. It is assumed that for brackish water containing several thousands ppms of NaCl, CDI may be advantageous over competitive methods (e.g., reverse osmosis). © 2009 American Institute of Chemical Engineers *AIChE J,* 56: 779–789, 2010

Keywords: water desalination, electrical double layer (EDL), capacitive deionization, activated carbon electrodes

Introduction

Population growth and the increase in the standard of living are continuously increasing the world's water demand. When adding this to the over exploitation and contamination of natural water resources by both industry and municipalities, one may reasonably anticipate that a global water crisis in the near future is inevitable. New clean water resources will have to be found or developed; otherwise, serious socio-economic problems will arise because of the lack of water in many parts of the world.

Fortunately, apart from irrigation in arid zones, water is not exhaustible, as is oil for instance. It is only contaminated, mostly because of the fault of the users. For instance, a too intensive usage of fresh water wells in coastal plains leads to the contamination of aquifers by salty water. Hence, water can be recycled by purification and desalination processes. The ultimate, unlimited source of water is of course the ocean. However, desalination of sea water, which contains about 40 g/l of NaCl, requires the use of too expensive processes.

Throughout the world, there are many sources of brackish water in which the salinity is, considerably, more than one order of magnitude lower than that of sea water. Hence, it may be very important to develop efficient processes for the desalination of brackish water, which may be much cheaper than the desalination of sea water.

The work reported herein involves an examination of several aspects of the desalination of aqueous NaCl solutions by the capacitive deionization (CDI) method. In this method, electrosorption and desorption are used according to the theory of the electrical double layer (EDL) of electrochemical systems,[1–4] while working within a potential window where electrochemical redox reactions are absent or negligible.

It is noteworthy that the energy demand per unit water volume for the CDI method, which is a process of removing salt, the minor component, from the water, is roughly proportional to the feed salt concentration. In the case of reverse osmosis, which is a process of removing water from the feed stream, the energy demand is much less dependent

Correspondence concerning this article should be addressed to D. Aurbach at aurbach@mail.biu.ac.il

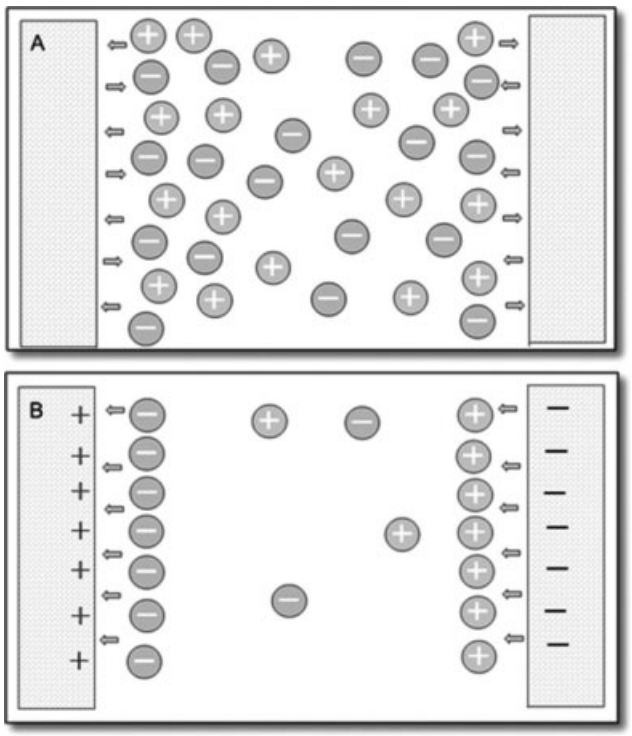

Figure 1. A scheme of the deionization process by an electroadsorption process.

(A) PZC Conditions. (B) A potential difference ΔE is applied. The arrows indicate water molecules oriented by the electrical field at the interfaces.

on the feed concentration. Thus, at lower concentrations, the electroadsorption method may become more economical than reverse osmosis, which presently dominates the market.

Activated carbon electrodes may reach specific surface areas higher than 2000 m^2/g (BET), while retaining very high electronic conductivity, in comparison with aqueous electronic conductivity, and displaying a wide electrochemical window (>1 V in aqueous systems and >5 V in selected nonaqueous solutions). These properties make them attractive for EDL or "super" capacitors, which exhibit much higher energy density than electrolytic capacitors, higher power density than rechargeable batteries,[5] and demonstrate impressive cycleability. (The only relevant interactions are electrostatic, hence, there are no chemical degradation reactions that lead to capacity fading, as found in rechargeable batteries). This combination of properties makes active carbon electrodes being suitable for the removal of ions from solutions.

The basic idea of CDI processes is illustrated in Figures 1a, b, which shows a cell with two identical electrodes, both are initially assumed to be at their potential of zero charge (PZC). Hence, ion adsorption is small in the absence of an electrical field (at the PZC). By applying the potential difference to the cell (Figure 1b), anions and cations are adsorbed on the oppositely charged electrodes, leaving a diluted solution in the cell. Then, a dose of desalted solution is driven out from the cell as a product, under the constant feed flow, being replaced with a dose of a fresh feed solution. In the next step, the electrodes are discharged back to the initial (PZC) potential, thus, desorbing the salt (the individual ions from the oppositely charged electrodes) out from the interfacial double layer region into the bulk liquid phase to obtain a concentrated solution, which is disposed as waste. Hence, properly designed two-electrode cells can be used as recyclable desalination devices.

In terms of flow directions, cell configuration, and electrical charging regimes, there can be several modes of design and operation of CDI devices. In this work, we deal with the flow-by (FB) mode, subdivided into continuous FB (CFB) and stopped FB (SFB) modes. The term flow by implies that the solution flows in parallel to the electrodes, not through them. Figures 2a, b (with detailed explanation therein) illustrate the elementary cell configuration for these operation modes. In the CFB mode, the salt solution flows at a constant rate through a narrow gap (physical gap or porous separator) between the two electrodes, shaped as thin slabs. The presence of a separator between the electrodes is necessary to prevent shorts between them. This is important especially when fibrous activated carbon electrodes are used. On charging the electrodes, ions are electroadsorbed. Consequently, the salt concentration in the pores of the electrodes and the separator between them is reduced. The constant flow pushes the desalted water out through the product outlet by replacement with the entering feed solution. Subsequently, the electrodes are discharged, leading to an increase in the solution concentration. The solution flow is now directed to the waste outlet, thus, completing a cycle of the desalination-regeneration process. With the SFB mode, the feed solution flow is interrupted for predetermined periods of time, after each charging or discharging step (which lasts till the current decays to zero or to a small but steady-state value), thus, allowing concentration equilibration across the cell, i.e., in planes perpendicular to the flow direction. The feed solution

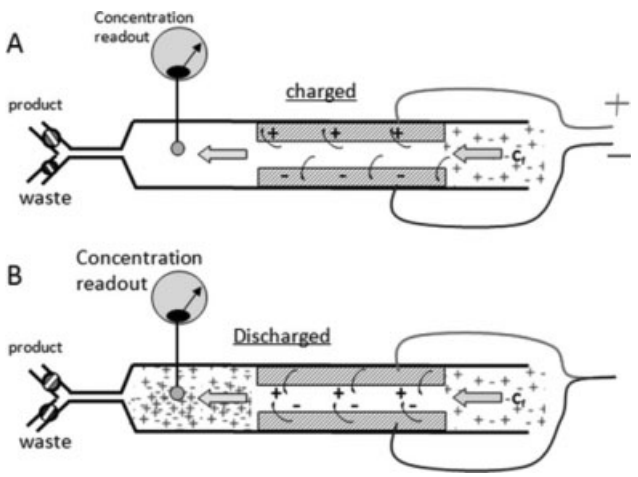

Figure 2. An illustration of a recyclable cell for the CDI process (based on EDL adsorption-desorption cycling).

(A) Desalination step: A potential difference of about 1.1 V is applied between the two electrodes. Ions are electrosorbed. The solution within the cell is desalinated and is driven out through the product outlet by the fresh feed solution (notice the valves on the left hand side); (B) Regeneration step; $\Delta E = 0$ (the two electrodes are short circuited), ions are electrodesorbed, and the resulting concentrate is driven out to the waste outlet.

then flows again toward the cell exit, thus, pushing out the desalted solution. This mode has the advantage of maximizing the separation per cycle, because ample time is allowed for the charging/discharging steps. However, the cycle durations may be long. This mode of operation is expected to be simpler for the purpose of study and interpretation, because the time domain for the ion removal from the solution (charging and ion diffusion to the electrodes' pores) is separated from the time domain for the collection of the product, namely, a desalted solution. Both CFB and SFB modes of operation are dealt with in this work.

It should be noted that studies of water desalination processes by electrochemical means are not new and have been dealt with during the last few decades. The idea of electrochemical water desalination was first raised in 1957 by Garten and Weiss.[6] This was followed by substantial experimental work by Murphy et al.[7,8] These authors emphasized the importance of the processes of the surface groups of carbon electrodes rather on their EDL capacitive behavior. Nowadays, numerous publications[2–4,9–11] have shown that the high electrical capacitance of porous activated carbon electrodes can be interpreted solely in terms of their EDL behavior. Several aspects of the EDL behavior of various electrodes and the influence of surface groups in determining the PZC were studied by Frumkin.[12] A unified thermodynamic theory for EDL and surface redox processes of activated carbon electrodes was formulated by Soffer.[4] The development of capacitive water deionization processes was further promoted by Farmer et al.,[13] based on aerogel carbon, a novel monolithic mesoporous carbon electrode possessing a surface area of 400–1000 m^2/g, developed by Pekala et al.[14] The engineering aspects of capacitive water deionization processes were studied by Andelman.[15] A review on capacitive water deionization processes covering the whole span from scientific work to commercialization status has been published recently by Oren.[16]

Despite the aforementioned work on electrochemical water desalination, there are still many aspects and issues that have not yet been addressed. Several of these aspects are dealt with herein, as listed below:

(a) Type of carbon electrodes, separators, and module design: The great majority of the previous studies involved the use of carbon aerogel as thin slabs, a few tenths of mm thick. This is an expensive and fragile carbonaceous material. In these studies (e.g., Refs. 13–15), the oppositely charged sheet electrodes were separated by empty gaps formed as a part of the module design.[13] In this work, we adopted a simpler and much more robust design in which flexible activated carbon cloth electrodes and macro/mesoporous separator in between are used. This simple approach enables the use of a wide variety of commercial or home made, inexpensive carbon electrodes and separators.

(b) Current collector: Although in previous studies[13] the current collector was titanium or its alloys, in this work, we successfully used a much cheaper current collector, made of flexible carbon film.

(c) Stopped flow regime: In this work, we employed, for the first time, the stopped flow mode of operation, which enables the separate study of charge and concentration transients.

(d) Concentration: Although most of the studies, including Farmer et al's, concentrated on desalination of diluted brackish water (<500 ppm NaCl), in this work, we covered also cases of concentrated brackish water (>5000 ppm NaCl). Studying this relatively wide concentration range, enables to estimate upper concentration limit of brackish water to which CDI is applicable as a competitive desalination method

(e) Charge efficiency: This crucial parameter, which is discussed herein, was not discussed or even mentioned in the literature since almost three decades ago (the mathematical expression of the charge efficiency in CDI processes was derived about 26 years ago[17]). As demonstrated recently,[18] the magnitude of the charge efficiency in CDI processes emerges from the behavior of each individual electrode in the reactor. In this article, its dependence on the experimental conditions is investigated for the first time.

We intend herein to further characterize model CDI processes, which continues earlier pioneering studies.[2,3,8,16,19,20] We describe herein deionization experiments with electrochemical cells based on activated carbon electrodes to which the CFB and the SFB modes of operation were applied. Several important parameters of CDI processes are discussed in detail. It should be emphasized that the results presented herein are far from demonstrating optimized water desalination, because the latter requires careful engineering optimization, which is beyond the scope of this work. However, the parameters and behavior measured and discussed herein may provide a good basis for such optimization and provide good guidelines for the design of practical, scaled up cells.

Experimental

The system's components

The system comprises a desalination reactor, programmable power supply, a conductometer, peristaltic pump, flow meters, and a storage bulb, as shown in Figure 3. The entire system is connected to a PC and controlled by a home-made program, based on LabView software, which controls the applied voltage and the solution flow rate, and reads and plots the conductivity and the current, vs. time. (A quite significant effort was devoted in developing the software–hardware interfacing and functionalities of this system). Sodium chloride solutions were circulated by a peristaltic pump via a tubing of minimal volume through the conductivity sensor and the electrochemical cell, as described schematically in Figure 3.

An arrangement for dissolving air pockets within the cell was as follows: prewetted air was bubbled into the 2-meters high storage bulb, which was also vented to the free atmosphere. This air-saturated solution (at 1 bar) was then passed through the CDI cell, held under a water column of $\sim$2 m. The solution entering the cell was, thus, only 80% saturated with any dissolved gas and could, therefore, dissolve the air trapped within the cell components. The removal of trapped air is important, because gas bubbles may impede the ionic current and the flow through each of the parallel slots within the separator sheets. In fact, we could observe the process at work while air bubbles gradually disappeared from the pressurized solution entering the cell.

When an inert atmosphere was needed (e.g., to eliminate any possible influence of oxygen reduction), the solutions were deaerated with nitrogen using the above setup.

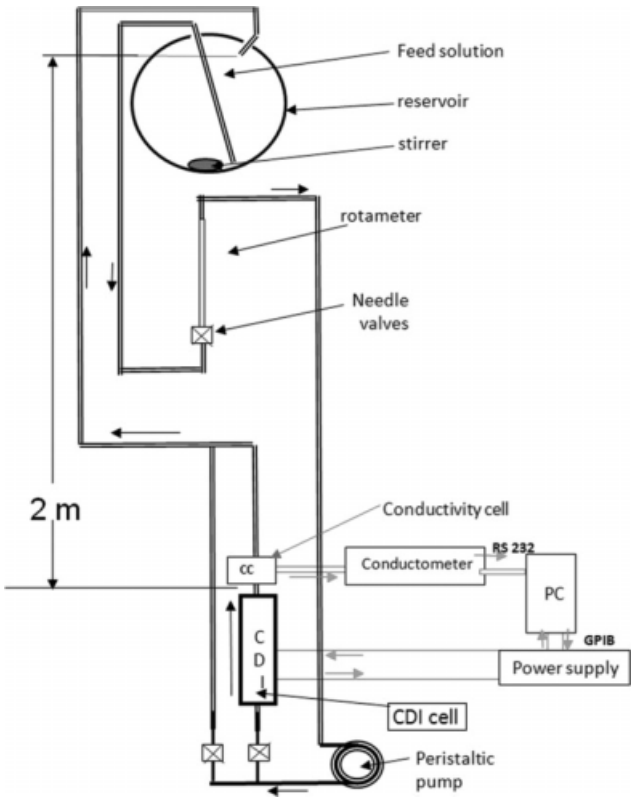

Figure 3. A scheme of the solution manipulation through the system's components.

A power supply from Keithley, Model 2440-5A Sink-Source-Meter, was used for applying its voltage to the cell for measuring the current. A conductometer, from Metrohm, Type 712, with a string-type output was digitized via the processing software and used for monitoring changes in salt concentration.

The CDI reactor

The reactor (Figure 4) was made of a stack of pairs of carbon cloth electrodes (Kynol CAT ACC-5092-15, 1500 m^2/g BET), 14 cm $\times$ 5 cm $\times$ 0.05 cm each, separated by a mesoporous, silica-filled polypropylene separator. This separator (Figure 4) was composed of two parallel sheets, 0.25-mm thick each, with a 1-mm thick separating gap between them. The gap was supported by ribs (indicated in Figure 4), along the separator sheets. The gap was the cell component responsible for the solution flow parallel to the electrode sheets. This enabled work in the FB operating mode (which we intend to explore in this work). Because of the mesoporous silica filling, in the separator walls, diffusion of solution components perpendicular to the electrodes' sheets was enabled. This, together with separating the electodes from each other, is the regular functions of the separator in electrochemical cells.

Each electrode was connected to a current collector layer made of an electrically conductive, carbon-based sheet. The current collector sheets protrude from the cell gasket, thus, having contact with flat brass rings pressed with screws and bolts (see the right side of Figure 4). In total, this reactor comprised 10 pairs of electrodes (20 carbon cloth sheets). The total carbon sheet mass of the cell was 14 g, and the total solution volume contained into the reactor was 80 ml. The volume of the freely flowing solution, about 40 ml was that contained in gaps (channels of flow) within the separator (Figure 4).

Types of experiments and data processing

We performed three series of experiments:

1. CFB mode with solutions containing 5500 ppm of NaCl;
2. CFB mode with solutions containing 550 ppm of NaCl; and
3. SFB mode with solutions containing 550 ppm of NaCl, applying different charge/discharge voltages.

It should be noted that solutions containing 5500 and 550 ppm NaCl are typical examples of brackish water of high and low salinity. Thereby, it was important to study both types of solutions. Unless otherwise specified, the following experimental conditions were applied. The pumping rate, 2 ml/min, was assumed to be low enough to minimize mixing; the applied charging potential was 1.1 V, which is slightly below 1.23 V, the thermodynamic potential window for water electrolysis and the discharging (regeneration) potential was 0 V.

Salt/charge efficiency

We define the salt/charge efficiency as the amount of salt adsorbed into the electrodes divided by the amount of electric charge (both in moles) passed through the cell.[16] This ratio is not necessarily unity, because the electric charge on the electrodes may be neutralized (from the solution side) not only by adsorption of counter ions[21] but also by desorption of co-ions, which have the same charge sign as that of

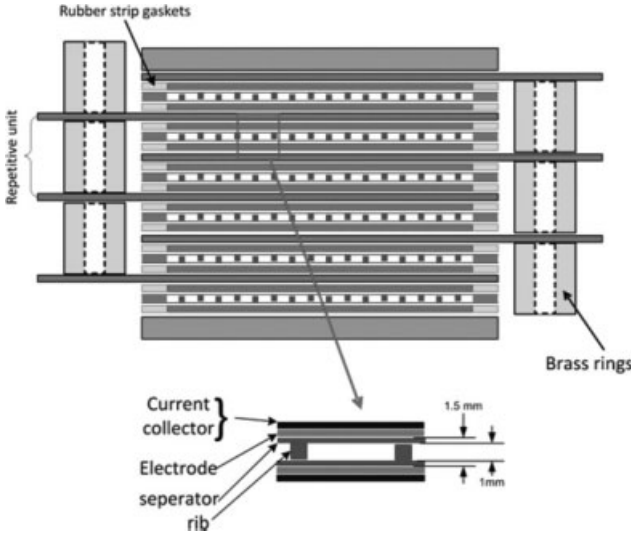

Figure 4. A scheme of the CDI reactor (the electrochemical cell for the water desalination process), structure, and configuration.

The solution flow direction is perpendicular to the "page plane."

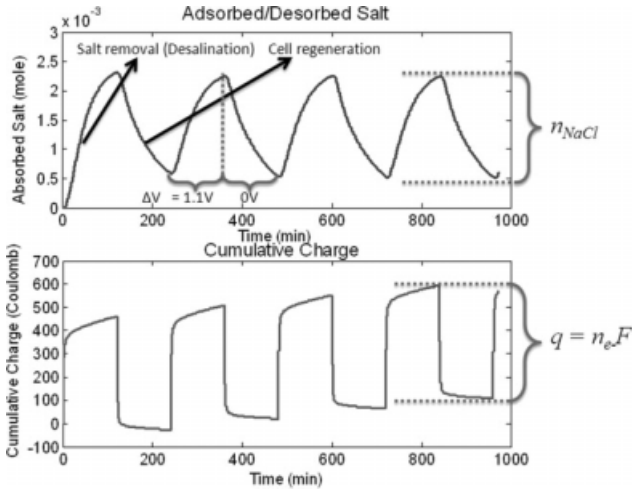

Figure 5. Typical salt adsorption and charge curves obtained by integration of concentration–time and current–time data during periodic charging/discharging curves.

Feed concentration is 5500 ppm NaCl.

the electrode.[22] This effect is very significant at potentials close to the PZC where cation adsorption and anion desorption (and vice versa) may occur simultaneously and equally. In fact, an electric charge may pass through the cell without any impact on desalination if the amount of cation released because of a positive charge admission to one electrode is equally adsorbed to the counter electrode due to the same (but opposite in sign) electric charge. In such a case, the salt/charge efficiency is zero. The phenomenon of ion release from one electrode with a simultaneous uptake by the counter electrodes at potentials not too far from the PZC was analyzed in detail elsewhere.[18]

The salt/charge efficiency is calculated as follows: The current is continuously integrated vs. time (see typical experimental results in Figure 5), giving the charge passed actually between the electrodes:

$$\int I \times dt = q \tag{1}$$

Translating the charge to molar values gives the following:

$$n_s = q/F \tag{2}$$

where F is the Faraday number. The solution conductivity, which was monitored continuously, is translated to changes in the salt concentration because of electroadsorption, compared with C_0, the salt concentration of the feed solution. Integration of the concentration changes over the volume of the solution that passes through the cell gives the amount of salt adsorbed (in moles), corresponding to the passage of charge as follows:

$$\int (C_0 - C_{out}) \times dV = n_{Nacl} \tag{3}$$

Hence, the salt adsorption (desalination) efficiency is given by

$$\eta = \frac{n_{Nacl}}{n_{e^-}} \tag{4}$$

Results and Discussion

Continuous flow-by mode

High Salt Concentration (5500 ppm NaCl) Capacity. Figure 5 shows typical experimental results in which a solution containing 5500 ppm NaCl is flowing through the CDI reactor operating in the CFB mode. The electrodes are charged and discharged (shorted) repeatedly, and the salt concentration at the outlet of the cell changes accordingly. The upper panel shows the periodic dependence of salt adsorption on time, obtained by the integration of the concentration with respect to time according to Eq. 4. The lower panel shows the cumulative charge (Eq. 1) vs. time for the same time scale. Figure 6 presents a typical response of the current and salt concentration vs. time, during periodic charge–discharge cycling (240 min/cycle) of the CDI reactor, with a continuous flow of a 5500 ppm NaCl feed solution. The applied potential was periodically changed from 0 to 1.1 V. As demonstrated, on charging, the NaCl concentration drops from 5500 to 4500 ppm. Such a drop is too small for desalination of practical significance (i.e., lowering the salt concentration to below 250 ppm to produce potable water). This minor change of only about 20% in concentration is because of the low ratio between the electroadsorbing surface area and the salt content in the feed solution. Obvious ways to increase this ratio is, of course, to use carbons of greater internal surface area per unit reactor volume and/or to minimize the void volume spaces containing bulk solution within the cell. As to increase the carbon electrode surface area, there are limitations to this approach, because of the conflict between high surface area (smaller pores) and high electroadsorption rate (larger, more permeable pores).[10]

A third approach to achieve potable water concentrations, besides optimizing electrode's surface area and porosity and minimizing void volumes, is limiting the feed concentration to values that are much below 5500 ppm NaCl. The optimal feed concentration for cells of the type described herein may be estimated roughly from results obtained in this work with

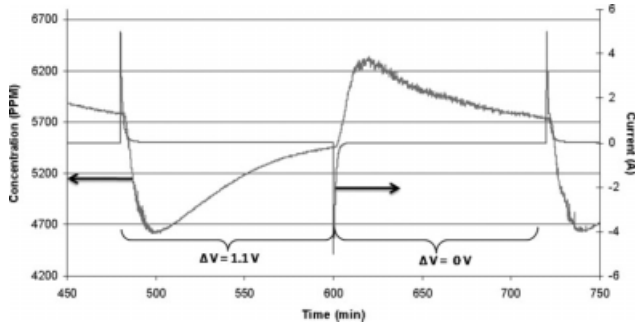

Figure 6. Changes in current and salt concentration, typically obtained on periodic polarization–depolarization of the CDI reactor, with a continuous flow of solution containing 5500 ppm of NaCl.

solutions containing low concentrations of NaCl. For instance, it was possible to reduce the NaCl concentration in solutions from 620 to 100 ppm NaCl by CDI in the system and operational mode described earlier (see Figure 10 and later discussion). Because the upper NaCl concentration limit for potable water is around 250 ppm, we assume that with the present reactor design (which is far from being optimized), it may be possible to desalinate brackish water containing 1000–2000 ppm NaCl, down to the level of potable water. At such feed concentrations, the CDI method, which is a process of minor component (salt) removal from the brine, may be energetically favorable over reverse osmosis, which, as mentioned in the introduction section, is a method of major component (water) removal from the brine. Optimization of the cell design may enable cost-effective desalination of brackish water with higher NaCl concentration (several thousands of ppm NaCl) down to the level of potable water, using CDI in a single pass operation (i.e., the feed solution filling the reactor undergoes a single charging step, after which it is totally removed as a product).

An important aspect of the efficiency of desalination relates to the energy consumption per unit volume of desalinated water. In contrast to brackish water desalination by reverse osmosis, where the salt concentration has a relatively small effect on the energy consumption, the energy of desalination by CDI is nearly proportional to the amount of ions in the solution. Hence, this latter method may be more cost effective for brackish water (namely solutions of relatively low salt concentration[16]) than other desalination methods. Finally, one can argue about the disadvantage of CDI related to the periodicity of the process. However, it should be easy to dispose the resulting concentrate and obtain a continuous supply of water by the use of an appropriate switching system and reservoirs for the product, potable water.

Kinetics. Another interesting phenomenon arising from Figure 6 is that following the potential step, the solution concentration rises and decays about 60–100-fold slower than the electrical current. This implies that improving the cycling rate (and, thus, the system's productivity) relates to the improvement of the mass transport at the solution side, while charging the electrode side is very fast. We, therefore, attempt to qualitatively understand which are the components that influence the time constants of the charging/discharging process. (Using appropriate available software, it is possible to treat the data quantitatively and develop models for the i, q, n, vs. t curves. However, this is beyond the scope of this work).

Figure 7 shows the essential cell components that play a role in the kinetic response of the CDI cell, as reflected by the time-dependent concentration presented in Figure 6. Because the channels within the separator are much wider than the interfiber gaps within the carbon cloth, the solution flows practically only through the rectangular cross-section tunnels within the separator (1-mm thick in the present cells). The starting point of the desalination cycle of operations is a short-circuited cell with a uniform salt concentration throughout. By applying a potential step, the charged active carbon electrodes attract counterions into their micropores and repel the co-ions, which move, under the electric field, toward the opposite electrodes. The adsorbed ions are

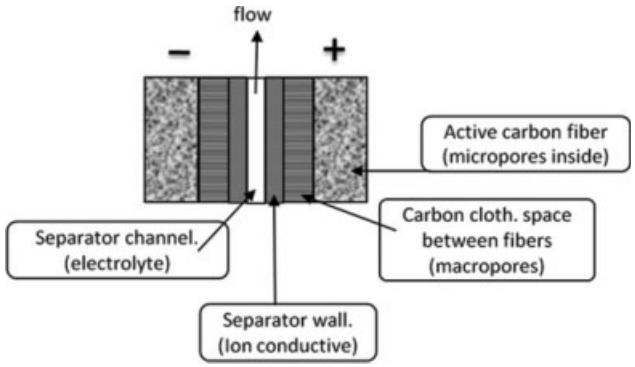

Figure 7. A schematic presentation of the cell components that play a role in its kinetic response (e.g., the concentration vs. time behavior seen in Figure 6).

taken off from the vicinity of the microporous carbon fibers, namely, from the macroporous space of the carbon cloth. The result is a depletion of ions from the macropores. The resulting concentration change is detected by the conductivity measurements only after a sequence of two time intervals. One interval is the time of diffusion, which is needed to reduce the concentration of the ions in the space between the macropores of the carbon cloth electrodes and the separator's channel. The second, consecutive interval is the time of solution transport from the channels of the separator out of the cell to the conductivity probe. In general, initial quantitative analysis of the transport situation in the reactors that we use can be carried out by calculating the Reynolds, Schmidt, and Peclet (Re, Sc, Pe) numbers.[23] Taking into account the width of the channels of the separator, the applied flow rate, the kinematic viscosity of the solutions measured, and the diffusivity of the ions involved, the Re number of the solution flow in all of the experiments described herein (in continuous flow operation mode) is about 0.14, indicating laminar flow. The relevant Sc numbers for Cl^- and Na^+ ions are about 490 and 750, while the Pe numbers for the same ions are 69 and 105, respectively. These high numbers mean that the rates of transport of ions by diffusion are negligible, when compared with their rate of transport by the flow of solution through the cell. The response of the solution containing 5500 ppm of salt to the potential step (electrodes' charging) is a fast change in concentration with a typical round peak (Figure 6). This peak-shaped behavior is explained by the high Sc and Pe numbers and is caused by the slow but prolonged transversal diffusion process from the micropores within the carbon cloth fibers, via the separator walls, into its channels, while the solution is flowing through. The concentration–time curve reflects the feed concentration for the period, during which the solution flows through the cell, while a constant potential difference is applied to the electrodes. The question now is how long this transient situation lasts and to what extent some sort of equilibrium conditions can be established? With the present cell and configuration, the electrical transient is two orders of magnitude shorter than the ionic one, which implies that there is a lot of room for improving the kinetics of ion transport in these cells and for optimizing the ratio between axial

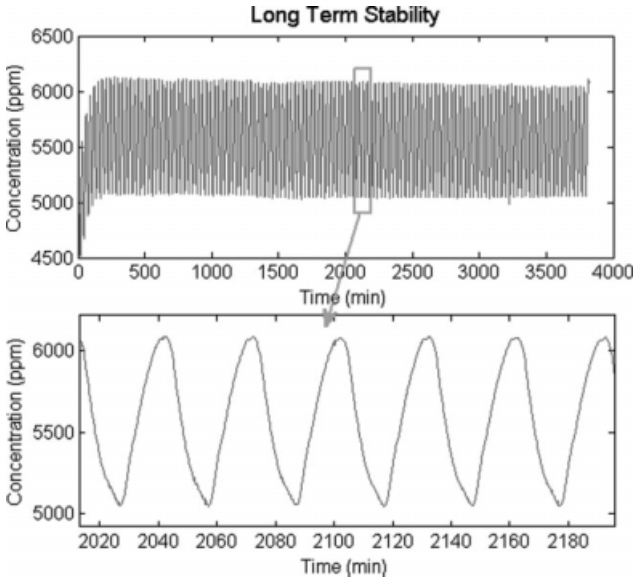

Figure 8. Periodic concentration profiles measured during repeated adsorption-desorption (charge-discharge) cycles, potential steps of 1.1 and 0 V, respectively, with a solution containing 5500 ppm of NaCl.

The duration of each cycle was 30 min, and the experiments were conducted continuously during 64 h with no change in the concentration profiles.

transport of ions by the solution flow and the transport of ions to the electrodes' pores (for their removal by CDI).

It should be noted that if there was no axial mixing in the CDI cell and if there was a very fast transversal diffusion and equilibration between the mobile solution within the separator and the stationary solution in the rest of the cell components (see Figure 7), the concentration–time plot (during discharge) should appear as a plateau for at least the following period of time, $\tau = V_f/(dV/dt)$ (which can be considered as the retention time, about 20 min, in our experiments; dV/dt being the solution flow rate) of the passage of one mobile solution volume (V_f, which is the volume of the separator that contains the flowing portion of the solution).

After that period, the concentration should gradually and asymptotically approach the concentration of the feed solution because of the diffusion of ions from the feed solution to the porous components of the cell (depleted from the ions, because the ions are adsorbed into the pores' walls). Because the solution flow is laminar and the ions diffusion rates are relatively slow, the possibility for axial mixing is low. Hence, the peak-shaped concentration–time response, seen in Figure 6, may indicate that the removal of ions from the flowing solution (a perpendicular transport by migration and diffusion) is too slow compared with the axial solution flow (through the channels of the separator). Consequently, it can be concluded that better results can be obtained using a ''flow through'' operational mode in which the solution is forced to flow through the porous electrodes and not in gaps between them.

Long-term Stability. Another important aspect measured herein, especially with the solutions containing a high salt concentration, was long-term stability. Figure 8 shows concentration profiles measured in an experiment in which adsorption/desalination–desorption cycles with potential steps of 1.1 and 0 V, about 30 min each, run repeatedly during 64 h. The results in Figure 8 show no change in the concentration amplitude, which is an indication of the stability of the electrodes. Hence, we expect that cells for water desalination based on activated carbon electrodes should be stable and should not require substantial maintenance related to their electrochemical operation.

Residual Currents. When dealing with water desalination by the CDI method, it is very important to address possible parasitic processes and leakage currents, which may interfere with the expected capacitive behavior of these systems. Figure 9 shows a curve of the charge (current integral over time) calculated per cycle, during a typical cycling experiment (described in the introduction). The slow rise of the charge seen in Figure 9 indicates that there is a charge accumulation within the system, superimposed on the charge measured during the course of the reversible desalination cycles. This is likely due to a minor water electrolysis process that takes place during the 1.1 V charging phase. This parasitic charge accumulation drops down with time, as seen in the figure. As such, the surface electro-oxidation of the active carbon electrode is also an option of a parasitic process in these systems. However, this option is more common in acidic solutions, which is not the present case. It should be noted that this minor (compared with the cyclic charging–discharging driving the desalination) charge accumulation process and its products are not detrimental to the water desalination process. However, it obviously involves some energy losses. In fact, it is not necessary to apply a potential difference as high as 1.1 V. Lower the potential difference, the lower is the possibility of parasitic processes. In addition, it is well known that active carbons of different origins and different thermal treatments are very different in their resistance to oxidation. Hence, the resistance of activated carbon electrode to oxidation may be improved (if at all necessary) by further thermochemical treatments.

Low Solution Concentration (620 ppm NaCl). Kinetic aspects associated with low feed concentrations. One might expect that at low salt concentrations, the concentration

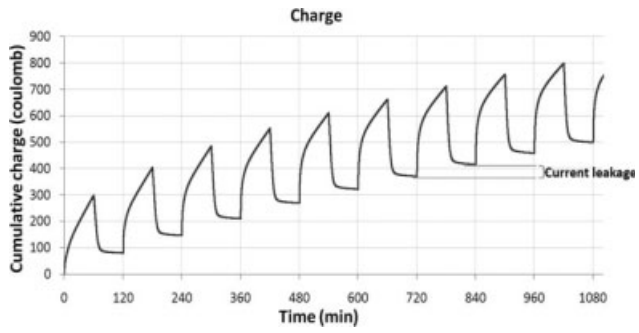

Figure 9. Typical charge profiles (*Q* vs. *t*) during repeated charge–discharge cycling of a solution containing 5500 ppm of NaCl.

The charge profiles were calculated during the adsorption (charging) steps, during which a potential difference of 1.1 V was applied to the electrodes.

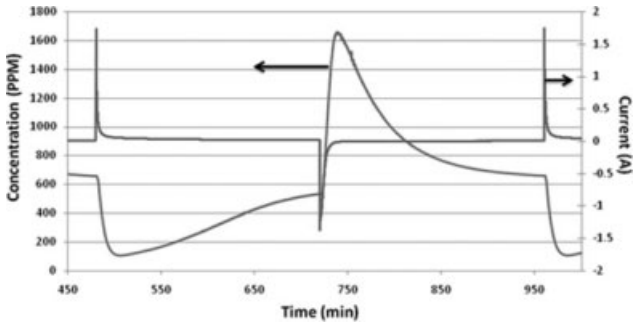

Figure 10. Concentration and charging current vs. time for the solution containing 620 ppm of NaCl.

Cycle duration: 480 min (adsorption–desorption process); solution flow rate: 2 ml/min.

transient time should be longer, compared with that of solutions of high salt concentration. However, Figure 10 shows that for solutions with about 10-fold lower NaCl content (620 ppm), the concentration transients (due to charge-discharge of the cell by potential steps) are not longer than those measured with the solutions containing 5500 ppm of salt, shown in Figure 6. In fact, the desorption curve seems to be relatively higher and sharper than the corresponding one for the 5500 ppm NaCl solution, presented in Figure 6. We anticipate that when the solution's concentration is low, there is no shielding effect of the ions in the various porous parts of the cell, and thus the electric field applied to the solutions due to the electrodes' polarization expands from the walls of the carbon cloth macropores (space between individual fibers >50 nm[11]) into the channels of the separator. This adds, in addition to diffusion, an ions flux forced by the electric field into the separator's channels (see Figure 7). Other features, evident from the presentation in Figure 10 are (a) the impressive six-fold drop in concentration of the deionized solution, down to 100 ppm NaCl during the adsorption steps (note that drinking water may bear up to 250 ppm NaCl); and (b) the concentration peaks during the desalination steps are lower and wider than those related to the regeneration steps, indicating that desalination is slower than regeneration (i.e., desorption of the ions back to the flowing solution). This surprising observation is due to the extreme dilution of the solution during the course of the deionization steps, leaving salt-depleted, poorly conductive space (filled with deionized water) in the vicinity of the carbon-solution interface. The asymmetry between the desalination and regeneration curves is clearly seen in Figure 10 and, as expected in light of this interpretation, is not observed in the experiments with the more concentrated solutions (Figure 6) because there, the concentration drop due to adsorption is not significant.

Comparison with literature at similar flow regimes and cell configuration. It should be both interesting and important to compare some results presented herein with results obtained in similar experiments published earlier by Farmer et al.[19] Their work also involved experiments using the CFB mode (although they did not call it as such) with solutions that freely flowed through gaps in parallel to the electrodes sheets. For solutions containing only several hundred ppm of NaCl, Farmer et al. also demonstrated an impressive five-fold reduction in the salt concentration on the desalination steps (from 550 to 100 ppm). Although the flow mode was the same for Farmer et al. system and our systems, the similarity between Farmer et al.'s results and the results presented herein is striking, because the operational parameters, cell design, and the type of carbon electrodes used by Farmer et al. were totally different. Figure 11 presents typical current and concentration transients from Farmer et al.'s work with CDI cells and feed solutions containing 550 ppm NaCl. As seen in this figure, the profiles of the concentration transients obtained by Farmer et al. are somewhat different from those shown in this work (compare Figures 10 and 11) and are closer to the shape of a plateau. This means that the axial mixing of desalted and feed solutions in Farmer et al.'s system was lower than the axial mixing in the experiments described herein. We attribute this advantage in Farmer et al.'s results to the effectively much longer path for the solution flow due to the serpentine-like configuration of the cells that they used,[19] where edge effects are less pronounced, while the cells used by us were relatively much shorter and wider. It is noteworthy that the phenomenon of much faster current transients, compared with the concentration transients, was also observed by Farmer et al. (Figure 11), indicating that this response is very typical of the CFB mode of operation. The difference between the concentration transient profiles measured by Farmer et al. and by us is most probably due to differences in the cell design used by the two groups. It is obvious that Farmer et al.'s use of a physical gap to separate between the two electrodes (instead of a separator, what was possible for the aerogel electrodes that they used) provides a higher ionic conductance between the two electrodes than in our case (the use of a mesoporous separator in this work). However, our advantage over the carbon aerogel used by Farmer et al. is in using generic carbon cloth electrodes that are flexible, much cheaper, and of greater (BET) surface area per unit electrode volume (this is in fact the main parameter that determines the ratio between the feed and the product concentrations that can be obtained by a single pass operation).

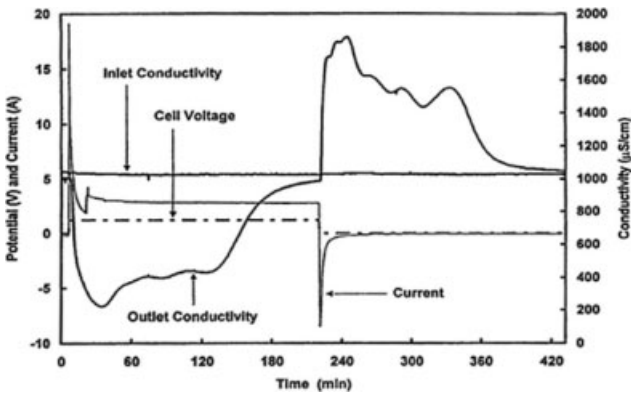

Figure 11. Results taken from the literature[19] obtained in experiments similar to those described in Figure 10: potential, current, and salt conductivity vs. time in a typical deionization/concentration cycle.

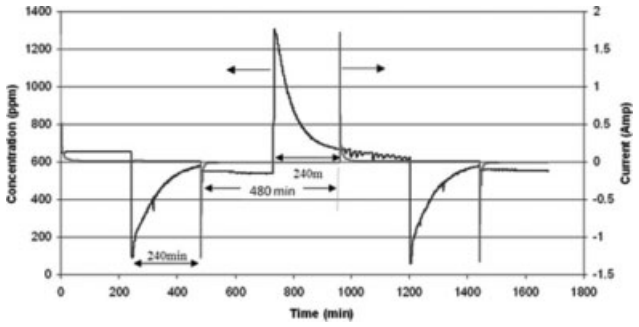

Figure 12. Presentation of data from a typical stopped flow experiment.

Currents and concentration profiles (translated from conductivity measurements) obtained with a solution containing 620 ppm at NaCl, potential steps at 1.1 and 0 V and a flow regime in which a potential step was applied during 480 min, but the solution was stopped from flowing during the first 240 min and was then forced to flow during the next 240 min of each cycle.

Stopped flow-by mode

In another set of experiments in the cells described earlier, pumping of the feed solutions into the cell was stopped during the application of each charge or discharge step for a predetermined, relatively long period of time (e.g., 220 min), to allow a full concentration equilibration during the course of the adsorption/desorption steps. The solution was then flowed (extracted) while the applied potential was still intact, through the conductivity cell for analysis. Figure 12 shows typical results of these experiments with a solution containing 620 ppm NaCl. Both the current and the concentration profiles (due to the application of potential steps) are presented. Although there is no doubt that with such a mode of operation (specially as the flow through the cell is laminar) the concentration profile inside the cell should be plateau shaped, the concentration profiles, thus, obtained (by the conductivity measurements) were all peak shaped (Figure 12). We can explain this peak-shape behavior by examining carefully the overall structure of the reactor, namely, the fact that the cross-section of the inlet and outlet are narrower than the cross-section of the cell. Thereby, the solution flow through the reactor is not uniform (yet, laminar everywhere therein). The solution flows relatively fast in the center and slowly near the perimeter. The peak-shape behavior, thus, obtained can be fully attributed to this nonuniform flow. Hence, a cell design with better dispensers may solve the problem (as is indeed found in further studies, beyond the scope of this article).

Parameters influencing deionization/charge efficiency

A series of experiments with solutions of two different salt concentrations were carried out using the CFB mode of operation, aiming at a study of the effect of cycle time on various parameters of the deionization processes. Table 1 summarizes the capacities and charge efficiencies for the experiments with solutions containing 550 ppm of NaCl and shows that decreasing the cycle time decreases the salt/charge efficiency of the system. This is reasonable, because at short cycle times, the concentration transient is cut prematurely, so that the salt diffusion from the stationary solution zone to the mobile zone is not yet completed. The fact that the salt/charge efficiency is much lower than 100%, even during prolonged cycling time (4 h), cannot be attributed to the EDL charging, because the electric current relaxation time is still much shorter than that of the concentration relaxation. It may relate to the coadsorption effect described in the experimental section (see Salt/Charge Efficiency, subsection).

Table 1. Capacitance and Charge/Salt Eficiency for Experiments with Solutions Containing 550 ppm NaCl

Cycle Time (min)	Charge Capacity (mmole/g)	Salt Capacity (mmole/g)	Salt/Charge Efficiency (%)
60	0.212	0.055	26
120	0.246	0.116	47
240	0.271	0.172	64

The potential steps were from 0 to 1.1 V.

Table 2 describes the same results as those of Table 1, but for the 10-fold 5500 ppm concentration. The 4-h cycle charge efficiency values are lower than those calculated for the diluted solution (as listed in Table 1). This again should be attributed to the coadsorption effect, which is stronger for more concentrated solutions (there are more of co-ions to desorb in parallel to adsorption of counter-ions). The charge efficiency for the 1-h and the 1/2-h cycle times are unexpectedly very low. This feature has to be further explored.

The last aspect dealt with herein relates to the efficiency of deionization vs. the charge consumption obtained in experiments with the stopped flow mode of operation. The solutions in these experiments contained 550 ppm of NaCl. We report herein about a series of experiments in which different potential steps were applied to the cells, starting with 0.2 V up to 1.2 V, with increments of 0.2 V after equilibration. The charge and deionization capacity in each step were calculated by dividing the changes measured in the charge accumulation and in the ion's adsorption (i.e., solution deionization translated to mmole units), by the potential step applied (0.2 V in these experiments). In addition, we calculated the deionization/charge efficiency as a function of the potential changes applied. The results are presented in Figure 13. As seen, and is indeed expected, the application of the first potential step of 0.2 V results in relatively low charge and deionization capacities. Then, further potential steps of 0.2 V result in the leveling off of the charge capacity and the peak-shape behavior of the deionization capacity and, consequently, of the charge/deionization efficiency. The maximum in the deionization capacity and in the related efficiency is measured when the potential step is changed from 0.6 to 0.8 V. This finding may indicate another important

Table 2. Capacitance and Charge/Salt Eficiency for Experiments with Solutions Containing 5500 ppm NaCl Solution

Cycle Time (min)	Charge Capacity (mmole)	Salt Capacity 2(mmole)	Salt/Charge Efficiency (%)
30	0.272	0.012	4
60	0.276	0.017	6
240	0.291	0.133	47

The potential steps were from 0 to 1.1 V.

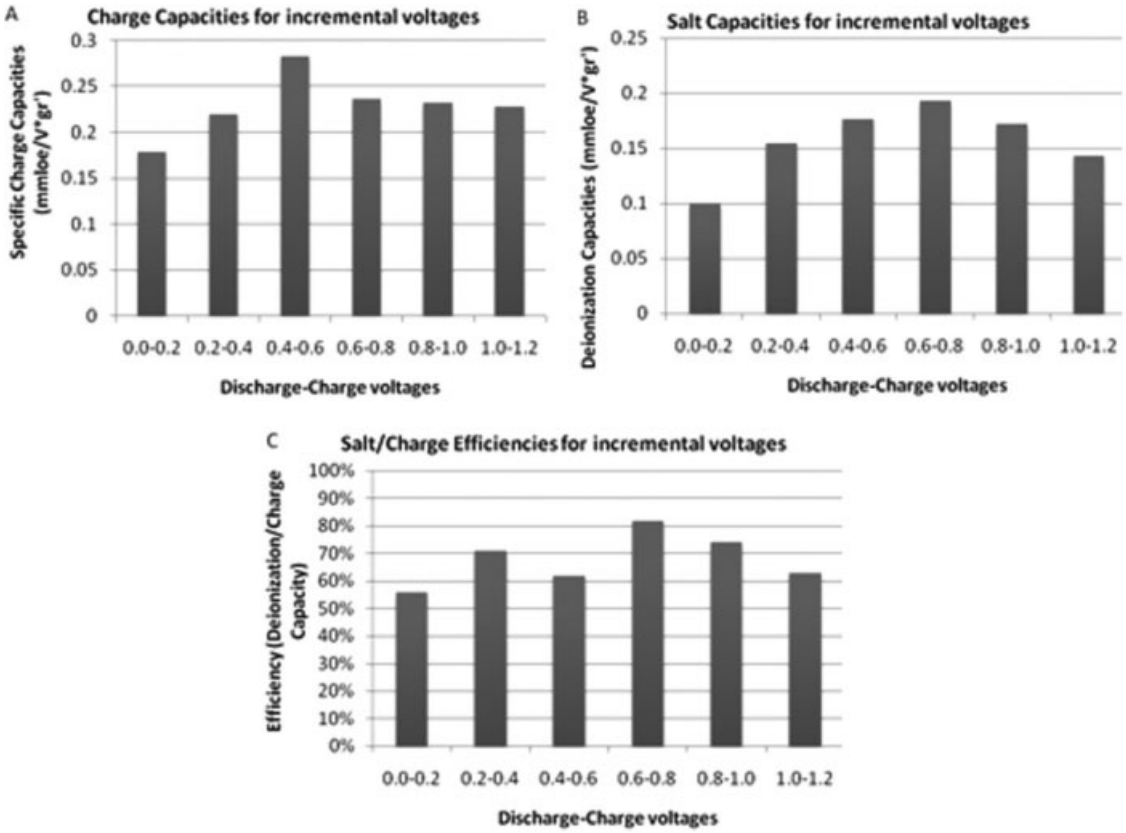

Figure 13. Specific charge capacities, specific deionization capacities (in mmole/V·g_{carbon}), and deionization/charge efficiency in experiments with a solution containing 550 ppm of NaCl.

A stop-flow mode in which the potential applied to the cell was stepped up in 0.2 V increments, followed by charge and deionization measurements. The capacities were calculated by dividing the changes in electric charged or ionic charge (translated to mmoles) by the potential changes (0.2 V). They are presented as specific values (per 1 g of carbon electrode material).

direction of optimization, i.e., the potential applied. At a first glance, one would suggest that in the CDI processes, the maximal potential that does not yet lead to water electrolysis should be applied. However, in term of energy efficiency, and hence specific operation costs, there may be an optimum in the potential applied that is lower that the maximal value (beyond which Faradaic reactions may take place). Indeed, further parallel studies revealed a quite complicated dependence of the charge/deionization efficiency of CDI processes on the applied potential.[18]

Conclusions

Water desalination by means of electroadsorption/desorption or CDI is unique and may be important and practical in the following aspects:

- Low energy demand involving neither phase nor temperature changes.
- Significant recovery of the invested capacitive electrical energy is possible.
- Maintenance treatments without chemical additives may be carried on electrochemically, i.e., without chemical additives, by applying high voltage (>1.3 V), which should *in situ* form the required redox and/or PH environment.

In this work, we studied the behavior of the CDI reactor not only for the most known and employed mode of CFB but also for the mode of SFB, where the dynamic and stationary parameters could be separated for simpler analysis.

On the basis of the experiments reported herein, we estimate that cost-effective production of drinking water from salty water solutions by single-step CDI processes may be limited to salt solution containing concentration of a few thousands ppm of NaCl (brackish water). The upper concentration limit may be further increased on increasing the ratio between the amount of reversibly electroadsorbed salt and the amount of salt contained in the bulk solution filling the meso- and macrovoids, and gaps between the electrodes.

This work demonstrated the use of cheap and relatively simple components of cells for CDI processes (compared with expensive aerogel carbon electrodes used in pervious similar studies). Another aspect of optimization relates to energy (and hence cost) efficiency: the potential applied to the cells should be determined based on maximal deionization/charge efficiency and not by the widest potential span in which the response remains fully capacitive (i.e., no parasitic reactions). Finally, this work is aimed at providing a qualitative picture of the main parameters that affect CDI processes. A natural follow-up step is a quantitative work and optimization of the parameters described herein by modeling, using appropriate and available software for calculations related to transport phenomena.

Acknowledgements

A partial financial support for this work was obtained from the Chief Scientist of the Israel Ministry of Industry and Commerce and the Mekorot Co. (within the framework of "Nofar" Program). Helpful discussions with Prof. Simon Brandon from the Faculty of Chemical Engineering, Technion (Israel Institute of Engineering) should be acknowledged as well.

Literature Cited

1. Conway BE. *Electrochemical Supercapacitors: Scientific Fundamentals and Technological Applications*, *Ch 6, 9*. New York, NY: Kluwer Academic, 1999.
2. Soffer A, Folman M. The electrical double layer of high surface porous carbon electrode. *J Electroanal Chem.* 1972;38:25–43.
3. Kastening B, Hahn M, Rabanus B, Heins M, zum Felde U. Electronic properties and double layer of activated carbon. *Electrochimica Acta*. 1997;42:2789–2799.
4. Soffer A. Electrocapillary equations and double-layer charge of reversible electrodes. *J Electroanal Chem.* 1972;40:153.
5. Nishino A. Capacitors: Operating principles, current market and technical trends. *J Power Sources*. 1996;60:137–147.
6. Garten VA, Weiss DE and Willis JB. A new interpretation of the acidic and basic structures in carbons. Ii. The chromene-carbonium ion couple in carbon. *Australian J of Chem.* 1957;10:309–328.
7. Murphy GW. "*Annual Report to the US Department of Interior*." (1958).
8. Murphy GW. "*R&D progress Report to the US Department of Interior*." (1966).
9. Salitra G, Soffer A, Eliad L, Cohen Y and Aurbach D. Carbon electrodes for double-layer capacitors-i. Relations between ion and pore dimensions. *J Electrochem Soc*. 2000;147:2486–2493.
10. Eliad L, Salitra G, Soffer A, Aurbach D. Ion sieving effects in the electrical double layer of porous carbon electrodes: Estimating effective ion size in electrolytic solutions. *J Phys Chem B*. 2001;105: 6880–6887.
11. Sing KSW, Everett DH, Haul RAW, Moscou L, Pierotti RA, Rouquerol J, Siemieniewska T. Reporting physisorption data for gas solid systems with special reference to the determination of surface-area and porosity (recommendations 1984). *Pure Appl Chem*. 1985; 57:603–619.
12. Frumkin AN. Lippmann equation. Comments on part 22 of paper on impedance of galvanic cells by timmer sluyters-rehbach and sluyters. *J Electroanal Chem.* 1968;18:328.
13. Tran TD, Farmer JC, Murguia L. Method and apparatus for capacitive deionization and electrochemical purification and regeneration of electrodes, US Patent 6309532, 2001.
14. Pekala RW, Mayer ST, Poco JF, Kaschmitter JL. *Mat. Res. Soc. Symp. Proc.* (1993).
15. Andelman DM. US Patent 6781817, 2004.
16. Oren Y. Capacitive deionization (cdi) for desalination and water treatment-past, present and future (a review). *Desalination.* 2008;228:10–29.
17. Oren Y, Soffer A. Water desalting by means of electrochemical parametric pumping.1. The equilibrium properties of a batch unit-cell. *J Appl Electrochem.* 1983;13:473–487.
18. Avraham E, Bouhadana Y, Soffer A and Aurbach D. Limitation of charge efficiency in capacitive deionization i. On the behavior of single activated carbon. *J Electrochem Soc*. 2009;156:95–99.
19. Farmer JC, Bahowick SM, Harrar JE, Fix DV, Martinelli RE, Vu AK and Carroll KL. Electrosorption of chromium ions on carbon aerogel electrodes as a means of remediating ground water. *Energy Fuel*. 1997;11:337–347.
20. Farmer JC, Fix DV, Mack GV, Pekala RW, Poco JF. Capacitive deionization of nacl and nano3 solutions with carbon aerogel electrodes. *J Electrochem Soc*. 1996;143:159–169.
21. Ettree LS. Nomenclature for chromatography. *Pure Appl Chem.* 1993;65:819–872.
22. Everett DH. Manual of symbols and terminology for physicochernical quantities and units, appendix ii: Definitions, terminology and symbols in colloid and surface chemistry. *Pure Appl Chem.* 1972; 31:577–638.
23. Perry RH, Green DW. *Perry's Chemical Engineers' Handbook*, New York: McGraw-Hill, 2008.

Manuscript received Nov. 2, 2008, revision received Apr. 22, 2009, and final revision received Jun. 8, 2009.